EasyChair Preprint

№ 15531

Mixed Time-State Dependent Distributed Event-Triggered Consensus Protocol of a DC Microgrids Cluster

Zaid Al-Tameemi, Tek Lie, Ramon Zamora and Frede Blaabjerg

December 5, 2024

Mixed Time-State Dependent Distributed Event-Triggered Consensus Protocol of a DC Microgrids Cluster

Zaid Hamid Al-Tameemi[1], T. T. Lie[1], R. Zamora[1] and F. Blaabjerg[2]
[1] Department of Electrical and Electronic Engineering, Auckland University of Technology, Auckland 1010, New Zealand
[2] Department of Energy Technology, Aalborg University, Aalborg, Denmark

Abstract. This paper introduces a novel mixed time-state dependent distributed event-triggered consensus protocol (MDETC) designed to notably minimize communication requirements among microgrids (MGs) within a cluster while mitigating Zeno behavior. Additionally, a fixed-time consensus algorithm, enhanced by a saturation function, is integrated into the secondary control level to augment the current convergence within the cluster. The Grey Wolf Optimizer (GWO) method is employed to adjust the parameters of proportional-integral (PI) controllers at the primary control layer, thereby enhancing the system's resilience to disruptions. The simulation results reveal that the proposed control technique outperforms existing strategies in the literature, particularly in reducing triggering instants and ensuring swift convergence of currents along with rapid voltage recovery under diverse operating conditions. A simulation involving a cluster comprising four DC MGs is conducted in the MATLAB environment to confirm the efficacy of the proposed control technique against alternative techniques.

Keywords: Clustered DCMGs, Current sharing, MDETC, and Voltage regulation.

1. Introduction

Microgrids (MGs) are small-scale electrical networks that consist of several interconnected distributed generators (DGs), energy storage systems (ESS), and end-use loads [1]. This idea has been proposed as a viable option for constructing a local grid using various renewable energy resources (RES)[2]. Multiple MGs, involving DC, AC, and combination DC-AC microgrids, have been used in the literature to integrate RES with ESS to meet the required demand [3]. However, the number of DC MGs is growing far quicker than that of traditional AC MGs. This results from reduced harmonics or frequency incompatibilities, coupled with the lack of need for synchronization in the isolated mode and the elimination of concerns related to reactive power regulation [4]. Clusters of MGs near one another can be connected to improve the DCMG's adaptability and reliability [5]. A MG cluster has vital benefits such as (i) increases the proportion of renewable energy used while simultaneously increasing the size of the area serviced by the power grid, (ii) improve the stability and reliability of microgrids clusters in the presence of power generation uncertainties besides load vacillations; and (iii) boosts the efficacy, flexibility, besides the economy of the entire cluster [5]. However, these MGs must be coordinated effectively to maximize the utilization of each MG's resources inside a cluster.

Various control schemes exist for managing MGs in clusters: centralized, decentralized, distributed, and hierarchical methods. Decentralized droop control, while used for power distribution and voltage stability, can result in issues like improper current distribution and voltage fluctuations [6]. Centralized control gathers data from all MGs but faces a single point of failure [7]. These challenges have led to solutions like distributed hierarchical and two-level control methods [8], [9], [10].

Previous control methods, such as time-triggered consensus, successfully achieved voltage regulation and power distribution in MG clusters but depended on fixed

schedules, consuming resources, and requiring reliable communication networks [11]. To tackle this issue, distributed event-triggered control (DETC), which significantly lessens the burden of communication, is proposed. In contrast to distributed time-triggered control (DTTC), DETC operates based on a predetermined trigger condition that dictates the sampling and transmission of data [12]. Supposedly, the triggering condition is met when the system's error arising from the discrepancy between the actual system measurements of the system and the measurements at the previous triggering instants surpasses a specific threshold. This initiates the communication among agents in the system, facilitating the exchange of information[13]. This control approach successfully connects data sampling and control measures to the system's measurements. Previous studies have examined This control method in the context of AC microgrids for various applications, involving voltage and frequency control of the AC MGs [14], demand response strategies [15], economic dispatch within the smart microgrids [16], besides reactive power control [17].

Furthermore, numerous research has applied DETC to control DC MGs [13], [18], [19], [20], [21], [22], [23], [24], [25]. In [26] sliding mode event-triggered control mechanism, based on a leader-follower consensus protocol is used manage voltage in DCMGs. Kalman filter is used for an event triggering function to estimate the voltage of the DC converter and then adjust the DC bus voltage in DC microgrids [27]. Furthermore, a distributed Event triggering consensus approach based on a fixed allowable error threshold is introduced in [18] to realise voltage consensus on DC bus and ensure precise current sharing among distributed generation units in a microgrid. However, this method necessitates continuous monitoring of bus voltage. In [28], a state-dependent triggering condition threshold addresses average voltage adjustment in addition to proportional load current distribution in a DC MG. Another state-dependent event triggering condition is proposed in [13] to tackle the consensus issue in the DC-link voltage coupled with the current sharing of DGs. A periodical event-triggered control approach is proposed in [19] to regulate DC-link voltage and distribute currents among DGs using a state-dependent triggering function. In [20], an event condition based on a fixed allowable error threshold is adopted to adjust voltage and ensure proper current distribution across DGs in DC microgrids. A multilayer event-triggered consensus protocol is introduced in the hierarchical control scheme's second and third layers in DC MG clusters [29]. The event-triggered consensus protocol in the second layer addresses the current distribution and voltage adjustment among ESSs, and the designed control structure in the tertiary layer regulates the global current sharing through the pinned ESS updates. A new DETC protocol [30], [31] addresses this by prioritizing accurate load current sharing and voltage regulation. It exchanges output current information solely between controllers, aided by a voltage observer.

However, these earlier studies encountered several challenges: they relied on state-dependent functions, which could potentially lead to Zeno behavior, indicating the excessive sensitivity of the Event trigger consensus algorithm to minor state changes in the system. Additionally, they employed infinite-time consensus at the secondary control level and overlooked the importance of proper PI controller selection, resulting in slower voltage recovery during critical conditions. Moreover, [30], [31] primarily focused on addressing DG connection challenges in closely located MGs, neglecting the complexities associated with coordinating microgrids across distant clusters.

To address these challenges, this study introduces a robust mixed time-state dependent distributed event-triggering algorithm, a fixed-time consensus protocol, and employs the Grey Wolf Optimizer (GWO). Recognizing the limitations of radial configuration, including complex control and management, as well as restricted power exchanges due to bus capacity constraints [32]. This research opts for a four-DC MGs cluster with a ring architecture. Simulation conducted in the MATLAB environment evaluates the efficacy of the proposed control methodology. This architectural choice offers enhanced reliability, flexibility, fault isolation, and voltage stability[33].

Key contributions:

1. Introduction of a Robust mixed time-state dependent distributed event-triggered consensus protocol (MDETC), which uniquely combines state-dependent and time-dependent elements [34] to reduce triggering events, eliminating Zeno behavior.
2. Implementation of a Fixed-Time Consensus Algorithm using a saturation function in the secondary control layer to limit control outputs, preventing cluster oscillations. This achieves faster current convergence and shorter settling times.
3. Utilization of GWO for precise current sharing and DC voltage regulation, even under challenging conditions like load changes, faults, and communication delays.
4. Consideration of operational challenges in coordinating MGs within a cluster is crucial. The proposed control approach effectively minimizes inter-MG communication, thereby reducing the risk of communication delays—an essential concern in Microgrid Clusters (MGCs). It also promotes the cluster's energy-efficient and sustainable operation.

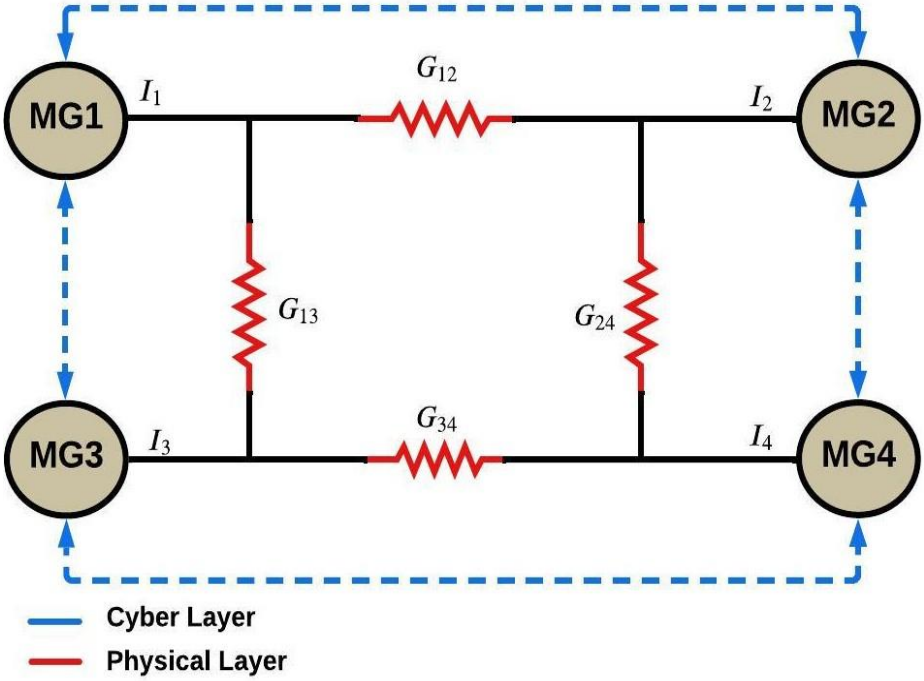

Fig.1. The configuration of DCMG Cluster.

2. Problem formulation

As depicted in Fig. 1, the DC MGs cluster is separated into two control layers: the cyber and physical layers.

2.1 Physical Layer

A graph comprises two specific finite sets: vertex ($\mathcal{V}$) and edges ($\mathcal{E}$). Each vertex represents multiple agents within a system, denoted as $\mathcal{V}e = \{1,2,\ldots,N\}$, while edges connecting paired agents are defined as $\mathcal{E}e \in \mathcal{V} \times \mathcal{V}$. In Fig. 1, each MG is equipped with two distributed generation units and DC-DC converters to adjust the system's voltage rating and maintain a constant current load. The physical structure of the cluster in Fig.1 could be represented as an undirected weighted graph $\mathcal{G}e(\mathcal{V},\mathcal{E},w)$, where microgrids (MGs) are the vertices and their power connections are the edges, respectively.

Precisely, $\mathcal{V}e = \{1,2,\ldots,N\}$ indexes N MG, and $\mathcal{E}e \in \mathcal{V} \times \mathcal{V}$ constitutes the edge set connecting MGs in the cluster. These MGs are linked through conductance lines, where edge weights (w) are assumed to be $1\Omega^{-1}$. It is crucial to point out that an edge $(i,j) \in \mathcal{E}e$, denotes that the data can be received by node *i* from node *j*. The adjacency matrix $\mathcal{A} = [G_{ij}] \in R^{N\times N}$ consists of non-negative elements with $G_{ij} = 1 \Leftrightarrow if an\ edge\ (i,j) \in \mathcal{E}e$ and $G_{e_{ij}} = 0$otherwise .The Laplacian matrix $\mathcal{L} = [l_{ij}] \in R^{N\times N}$ can be expressed as $l_{ij} = -g_{ij}, i \neq j$, and $l_{ii} = \sum_{j=1,j\neq i}^{N} G_{ij}$. Additionally, it is worth mentioning that $\mathcal{D} = diag\{G_{11}, G_{22}, \ldots, G_N\}$.

2.2 Cyber Layer

Graph theory visually represents communication networks within microgrid clusters [35]. This subsection outlines the communication network topology among MGs in the cluster using an undirected graph. Consider a cluster comprising N interacting MGs, where a weighted undirected graph is termed as $Gc(\mathcal{V},\mathcal{E})$, with $\mathcal{V} = \{1,2,\ldots,N\}$ symbolizing the index set of *N* microgrids, and $\mathcal{E} \in \mathcal{V} \times \mathcal{V}$ defining the edges set connecting the microgrids (MGs). An edge $(i,j) \in \mathcal{E}$ denotes that the data can be received by node *i* from node *j*. The adjacent matrix $\mathcal{A} = [a_{ij}] \in \boldsymbol{R}^{N\times N}$ contains non-negative elements with $a_{ij} = 1, if\ \ (i,j) \in \mathcal{E}$and $a_{ij} = 0$ otherwise. The Laplacian matrix $\mathcal{L}c = [l_{ij}] \in \boldsymbol{R}^{N\times N}$ can expressed as $l_{ij} = -a_{ij}, i \neq j$, and $l_{ii} = \sum_{j=1,j\neq i}^{N} a_{ij}$. Moreover, it should be noted that $\mathcal{D} = diag\{a_{11}, a_{22}, \ldots, a_{NN}\}$.

3. The Main Control Objectives

Inspired by [30], the control objectives for multiple microgrids (MGs), including proportional current sharing and average voltage regulation, are formulated as follows:

$$\lim_{t\to\infty}\left(\frac{I_i}{I_{ci}} - \frac{I_j}{I_{cj}}\right) = 0 \qquad \text{for all } i,j \in \mathcal{V}e \tag{1}$$

where, $I_{ci}$and I_{cj} symbolize the maximum loading capabilities of MG_i and MG_j in a cluster, respectively, which are supposed to be higher than zero. Eq. (2) specifies how to adjust the overall average voltage of the constructed cluster in Fig.1 to match Vdc_{ref} in a steady state. Essentially, $\bar{\mathrm{V}}\mathrm{dc} - Vdc_{ref}$ should equal zero.

$$\bar{V}dc = \frac{1}{n}\sum_{i=1}^{n} Vdc_i = Vdc_{ref} \tag{2}$$

In this context, $\bar{\mathrm{V}}\mathrm{dc}$ denotes the average voltage observer of the MG cluster, $\mathrm{Vdc_i}$ refers to the voltage of $\mathrm{MG_i}$ and Vdc_{ref} is the standard voltage of the DC MG cluster, as revealed in Fig.1.

4. Problem Formulation

4.1 A Modified Fixed-Time Consensus Algorithm

A fixed-time consensus algorithm utilizing saturation function (sat) is employed in the second control layer, as indicated by Eq. (3), to attain fast current convergence speed along with less voltage recovery time. The voltage information can be inferred by determining the error the microgrid's current, which is subsequently employed to determine the cluster's reference voltage (V_{ref}) as described in Eq. (4). This control approach is employed in multiple MGs with a new proposed threshold value based on the cluster situation, as illustrated in Fig.2.

$$\hat{u}_i = k_1 sat(\hat{\varphi}_{Li})^m + k_2 sat(\hat{\varphi}_{Li})^n \tag{3}$$

$$V_{ref} = \Delta V_v + \Delta V_i \tag{4}$$

where, m , n , k_1 *and* k_2 indicate control coefficients that need to be within a range of *1* for k_1 *and* k_2 along with $m = 1/n$. Integrating the Eq. (5) with the gain control factor (Ki).

According to Eq. (4), the two components of Vref can be calculated depending on the available currents at the most recent triggering instants, as expressed in Eq. (5).

$$\hat{\varphi}_{Li} = a_{ij}\sum_{j\in i}\left(\frac{\hat{I}_i(t)}{I_{ci}} - \frac{\hat{I}_j(t)}{I_{cj}}\right) \quad where\ \ t \in (t_k^i, t_{k+1}^i) \tag{5}$$

By substituting Eq. (5) into Eq. (3), the estimated current error $(\hat{u}_i)$ can be calculated as shown in Eq. (6).

$$\hat{u}_i = k_1 sat(a_{ij} \sum_{j\in i}(\frac{\hat{I}_i(t)}{I_{ci}} - \frac{\hat{I}_j(t)}{I_{cj}}))^m + k_2 sat(a_{ij} \sum_{j\in i}(\frac{\hat{I}_i(t)}{I_{ci}} - \frac{\hat{I}_j(t)}{I_{cj}}))^n \quad (6)$$

where, $\hat{I}_i$ *and* $\hat{I}_j$ indicate the most recent triggering instance values of the microgrids (MG) currents. By multiplying Eq. (6) with the gain control (K_i), and integrating the result, the current correction factor (ΔV_i) can be calculated as shown in Eq. (7).

$$\Delta V_i = K_i \int_0^t \hat{u}_i \, dt \quad (7)$$

Another component of V_{ref} could be determined by calculating the locally measured voltage regulation ($\hat{\bar{V}}\mathrm{dc_i}$), which is obtained by summing the local voltage of the first microgrid($\mathrm{MG_i}$)and integrating the result of multiplying Eq. (6) by the gain control (K_t).

$$\hat{\bar{V}}dc_i = Vdc_i + \hat{\varphi}_{Vi} \quad (8)$$

$$\hat{\varphi}_{Vi} = K_t \int_0^t \hat{u}_i \, dt \quad (9)$$

$$\hat{u}_v = \hat{\bar{V}}dc_i - Vdcref \quad (10)$$

$$\hat{u}_v = (Vdc_i + K_t \int_0^t \hat{u}_i\,) - Vdc_{ref} \quad (11)$$

$$\Delta V_v = K_v \cdot \hat{u}_v = K_v \cdot (Vdc_i + K_t \int_0^t \hat{u}_i\,) - Vdc_{ref}) \quad (12)$$

Therefore, both Eqs. (7) and (12) are substituted into Eq. (4) to supply the reference voltage that is delivered to the primary control layer of each MG in the cluster, as expressed in Eq. (13).

$$V_{ref} = (Vdc_i + Kt \int_0^t \hat{u}_i \; dt) - Vdc_{ref})\, K_v + K_i \int_0^t \hat{u}_i \; dt \quad (13)$$

$$\dot{V}_{ref} = -K_v \cdot \hat{u}_v - K_i \cdot \hat{u}_i \quad (14)$$

4.2 Lyapunov Stability

Based on Eq. (14) and using the principle of Lyapunov equation, Eq. (15) can be obtained.

$$W = \frac{1}{2} {V_{ref}}^T L_e V_{ref} \rightarrow \dot{W} = {V_{ref}}^T L_e \dot{V}_{ref} = -I(K_v \cdot \hat{u}_v + K_i \cdot \hat{u}_i) = -(IK_v\hat{u}_v + IK_i\hat{u}_i) \quad (15)$$

In order to acquire the output current of MG, the error of the current in Eq. (5) can be rearranged to obtain the current as in Eq. (16).

$$I = \frac{\varphi_{Li}}{L_c I_c^{-1}} \quad (16)$$

The connection between the error in real time microgrid's currents allocation and event-triggered currents allocation must be established, as illustrated in Eq. (17).

$$\begin{cases} ei(t) = \frac{I_i(t_{k+1})}{I_{ci}} - \frac{\hat{I}_i(t_k)}{I_{ci}} \rightarrow \frac{\hat{I}_i(t_k)}{I_{ci}} = \frac{I_i(t_{k+1})}{I_{ci}} - ei(t) \\ ej(t) = \frac{I_j(t_{k+1})}{I_{cj}} - \frac{\hat{I}_j(t_k)}{I_{cj}} \rightarrow \frac{\hat{I}_j(t_k)}{I_{cj}} = \frac{I_j(t_{k+1})}{I_{cj}} - ej(t) \end{cases} \quad (17)$$

Then, Substituting Eq. *(*17*)* into Eq. (5) produces Eq. (18).

$$\hat{\varphi}_{Li} = a_{ij} \sum_{j\in i}(\frac{I_i(t)}{I_{ci}} - ei(t) - \frac{I_j(t)}{I_{cj}} + ej(t)) \quad (18)$$

Eq. (18) is further organized and rearranged to make it in terms of the Laplacian matrix so that Eq. (19) can be obtained.

$$\hat{\varphi}_{Li} = \varphi_{Li} - L_c e(t) \rightarrow \hat{\varphi}_{Li} = \varphi_{Li} + L_c e(t) \quad (19)$$

Eq. (19) is inserted into Eq. (16) to obtain Eq. (20), which is subsequently substituted into Eq. (15) to obtain Eq. (21).

$$I = \frac{\hat{\varphi}_{Li}}{L_c I_c^{-1}} + \frac{L_c e(t)}{L_c I_c^{-1}} = \frac{\hat{\varphi}_{Li}}{L_c I_c^{-1}} + \frac{e(t)}{I_c^{-1}} \quad (20)$$

$$\dot{W} = -\left(\frac{\hat{\varphi}_{Li}}{L_c I_c^{-1}} + \frac{e(t)}{I_c^{-1}}\right)(K_v\hat{u}_v + K_i\hat{u}_i) = -K_v\hat{u}_v \frac{\hat{\varphi}_{Li}}{L_c I_c^{-1}} - K_v\hat{u}_v \frac{e(t)}{I_c^{-1}} - K_i\hat{u}_i \frac{\hat{\varphi}_{Li}}{L_c I_c^{-1}} - \frac{e(t)}{I_c^{-1}} K_i\hat{u}_i \quad (21)$$

Depending on the derived Lyapunov function shown later in the section and a comparison with the root of inequality $\mp xy \leq \left(\frac{b}{2}\right)x^2 + \left(\frac{1}{2b}\right)y^2$, Eqs. (22) and (23) are obtained:

$$K_v\hat{u}_v \frac{\hat{\varphi}_{Li}}{L_c I_c^{-1}} \leq \frac{K_v b}{2L_c I_c^{-1}} {\hat{u}_v}^2 + \frac{K_v}{2bL_c I_c^{-1}} {\hat{u}_i}^2 \quad (22)$$

$$K_i\hat{u}_i \frac{\hat{\varphi}_{Li}}{L_c I_c^{-1}} \leq \frac{K_i}{2L_c I_c^{-1}} {\hat{u}_i}^2 \quad (23)$$

For a seek of simplicity, $\hat{\varphi}_{Li}$ *is assumed to be* $\hat{u}_i$

$$-K_v\hat{u}_v\frac{e(t)}{I_c^{-1}} \leq \frac{K_v b}{2I_c^{-1}}\hat{u}_v{}^2 + \frac{K_v}{2bI_c^{-1}}e(t)^2 \quad (24)$$

$$\frac{e(t)}{Ic^{-1}}K_i\hat{u}_i \leq \frac{K_i b}{2I_c^{-1}}\hat{u}_i{}^2 + \frac{K_i}{2bI_c^{-1}}e(t)^2 \quad (25)$$

Eqs. (22-25) are then substituted into Eq. (21) to obtain Eq. (26).

$$\dot{W}t \leq \frac{K_v b}{2L_c I_c^{-1}}\hat{u}_v{}^2 + \frac{K_v}{2bL_c I_c^{-1}}\hat{u}_i{}^2 + \frac{K_v b}{2I_c^{-1}}\hat{u}_v{}^2 + \frac{K_v}{2bI_c^{-1}}e(t)^2 + \frac{K_i b}{2I_c^{-1}}\hat{u}_i{}^2 + \frac{K_i}{2bI_c^{-1}}e(t)^2 + \frac{K_i}{2L_c I_c^{-1}}\hat{u}_i{}^2 \quad (26)$$

By rearranging Eq. (26), the Lyapunov function can be obtained as follows (see Eq. (27)):

$$\dot{W}t \leq (\frac{K_v b}{2L_c I_c^{-1}} + \frac{K_v b}{2I_c^{-1}})\hat{u}_v{}^2 + (\frac{K_v}{2bL_c I_c^{-1}} + \frac{K_i b}{2I_c^{-1}} + \frac{K_i}{L_c I_c^{-1}})\hat{u}_i{}^2 + (\frac{K_v}{2bI_c^{-1}} + \frac{K_i}{2bI_c^{-1}})e(t)^2 \quad (27)$$

From Eq. (27), the new error threshold can be defined as shown in Eq. (28):

$$e(t)^2 \geq \frac{\left(\frac{K_v b}{L_c} + \frac{K_v b}{1}\right)\hat{u}_v{}^2 + \left(\frac{K_v}{bL_c} + \frac{K_i b}{1} + 2\frac{K_i}{L_c}\right)\hat{u}_i{}^2}{\left(\frac{K_i + K_v}{b}\right)} \quad (28)$$

It is noticeable that Eq. (28) can be further simplified by incorporating β to derive Eq. (29).

$$e(t)^2 \geq \sigma\left(\frac{K_v b + L_c K_v b}{\frac{K_i + K_v}{b}L_c}\right)\hat{u}_v{}^2 + \sigma\left(\frac{K_v + L_c K_i b^2 + 2K_i b}{(K_i + K_v)L_c}\right)\hat{u}_i{}^2 + \beta) \quad (29)$$

In Eq. (29), a state-dependent function (SDF) is derived. By combining the best features of SDF and the time-dependent triggered function (TDF), a mixed-dependent function (MDF) is achieved. The MDF protocol prevents excessive triggering during consensus and eliminates Zeno behavior. Compared to other triggering methods, MTF has been found to offer superior trigger performance with the fewest total events [36]. To harness the benefits of this protocol, a time-dependent term is introduced into Eq. (29) to optimize DETC's triggering instants in a cluster. Thus, Eq. (29) is further modified as follows in Eq. (30):

$$e(t)^2 \geq \sigma\left(\frac{K_v b + L_c K_v b}{\frac{K_i + K_v}{b}L_c}\right)\hat{u}_v{}^2 + \sigma\left(\frac{K_v + L_c K_i b^2 + 2K_i b}{(K_i + K_v)L_c}\right)\hat{u}_i{}^2 + \beta + ce^{-\rho t} \quad (30)$$

The value of σ , ρ, c, and b should be less than 1. These parameters need to be chosen appropriately depending on the system situation with an acceptable range (0-0.999) that makes the error threshold more robust and less sensitive to small variations in the cluster as they impact on increasing or decreasing threshold value of the error which leads to improper triggering instants in each MG. The error, which arises from difference between the actual microgrids currents and those stored from the previous triggering instance, which is represented by $e_i(t) = I_i(t) - \bar{I}_i(t_k)$, will be compared with the threshold defined in Eq. (30). If it exceeds this threshold, it will be triggered, as explained in Fig.2. It should be noted that the use of β in Eq. (30) results in the creation of a little margin for the growth of the error. As a result, the Zeno phenomenon is prevented from happening, and the event condition is no longer set off by minor errors [24].

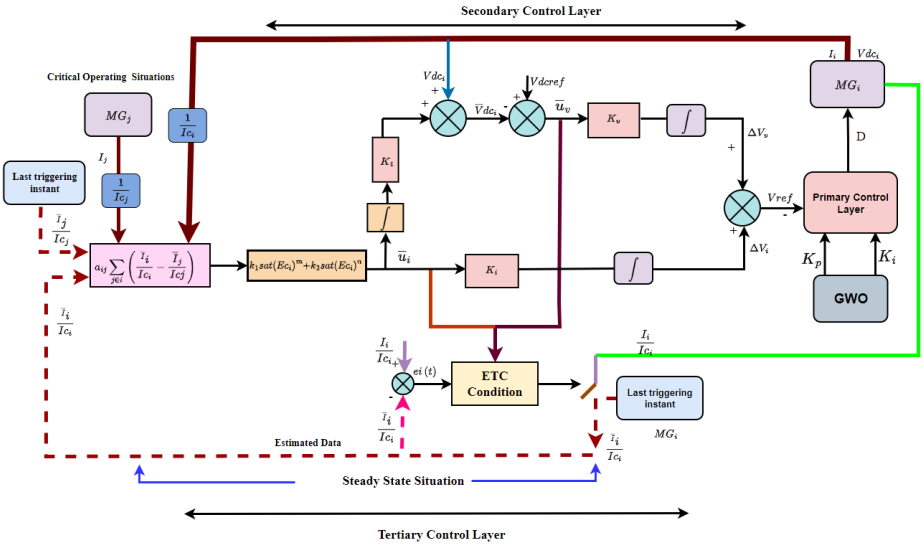

Fig.2 Proposed control approach

A Modified Fixed-Time Consensus Algorithm

Set the values of $\boldsymbol{k_1}$, $\boldsymbol{k_2}$, $\boldsymbol{m}$,and $\boldsymbol{n}$
Import currents (I_i *and* I_j) from Microgrids
  For each $\boldsymbol{MG_i}$
    For each neighbouring $\boldsymbol{MG_j}$
      $\hat{\varphi}_{Li} = a_{ij} \sum_{j\in i}(\frac{\hat{I}_i(t)}{I_{ci}} - \frac{\hat{I}_j(t)}{I_{cj}})$
  Compute estimated current error
  $\hat{\boldsymbol{u}}_{\boldsymbol{i}} = \boldsymbol{k_1 sat}(\hat{\varphi}_{Li})^{\boldsymbol{m}} + \boldsymbol{k_2 sat}(\hat{\varphi}_{Li})^{\boldsymbol{n}}$
  Compute voltage error
  $\hat{\varphi}_{Vi} = K_t \int_0^t \hat{u}_i \, dt$
  Compute average bus voltage
  $\hat{\bar{\boldsymbol{V}}}\boldsymbol{dc_i} = \boldsymbol{Vdc_i} + \hat{\boldsymbol{\varphi}}_{\boldsymbol{Vi}}$
  Compute voltage regulation error
  $\hat{\boldsymbol{u}}_{\boldsymbol{v}} = \hat{\bar{\boldsymbol{V}}}\boldsymbol{dc_i} - \boldsymbol{Vdc_{ref}}$
  Compute correction factors
    $\Delta \boldsymbol{V_i} = \boldsymbol{K_i} \int_0^t \hat{\boldsymbol{u}}_{\boldsymbol{i}} \, \boldsymbol{dt}$
    $\Delta \boldsymbol{V_v} = \boldsymbol{K_v} \cdot \hat{\boldsymbol{u}}_{\boldsymbol{v}} = \boldsymbol{K_v} \cdot (\boldsymbol{Vdc_i} + \boldsymbol{K_t} \int_0^t \hat{\boldsymbol{u}}_{\boldsymbol{i}}) - \boldsymbol{Vdc_{ref}})$
  Compute the reference voltage
  $\boldsymbol{V_{ref}} = \Delta \boldsymbol{V_v} + \Delta \boldsymbol{V_i}$

5. Results And Discussion

The model is employed to evaluate the superiority of the mixed time-state dependent distributed event-triggered consensus (MDETC) protocol compared to previous control strategies, the four DC-MGs cluster in MATLAB, as depicted in Fig. 1. The MGs are interconnected through tie lines represented as 1 Ω resistances. Each MG features two DG units arranged in tandem. Additionally, DC-DC buck converters in each MG lower the output voltage from 100V to 48V for local loads. Fig. 3 illustrates the key components of each microgrid in the cluster, and Table 1 provides detailed MG information. Furthermore, the PI-controllers'parameters in each primary (local) control layer are determined using the GWO, as explained in [37]. Fig. 1 shows that each MG's controller exchanges local information solely with closely related MGs, reducing communication overhead compared to prior studies. This interaction enables the derivation of the Laplacian matrix as follows:

$$\mathcal{L}_e = \begin{bmatrix} G_{11} & G_{12} & G_{13} & G_{14} \\ G_{21} & G_{22} & G_{23} & G_{24} \\ G_{31} & G_{32} & G_{33} & G_{34} \\ G_{41} & G_{42} & G_{43} & G_{44} \end{bmatrix} = \begin{bmatrix} 2 & -1 & -1 & 0 \\ -1 & 2 & 0 & -1 \\ -1 & 0 & 2 & -1 \\ 0 & -1 & -1 & 2 \end{bmatrix}$$

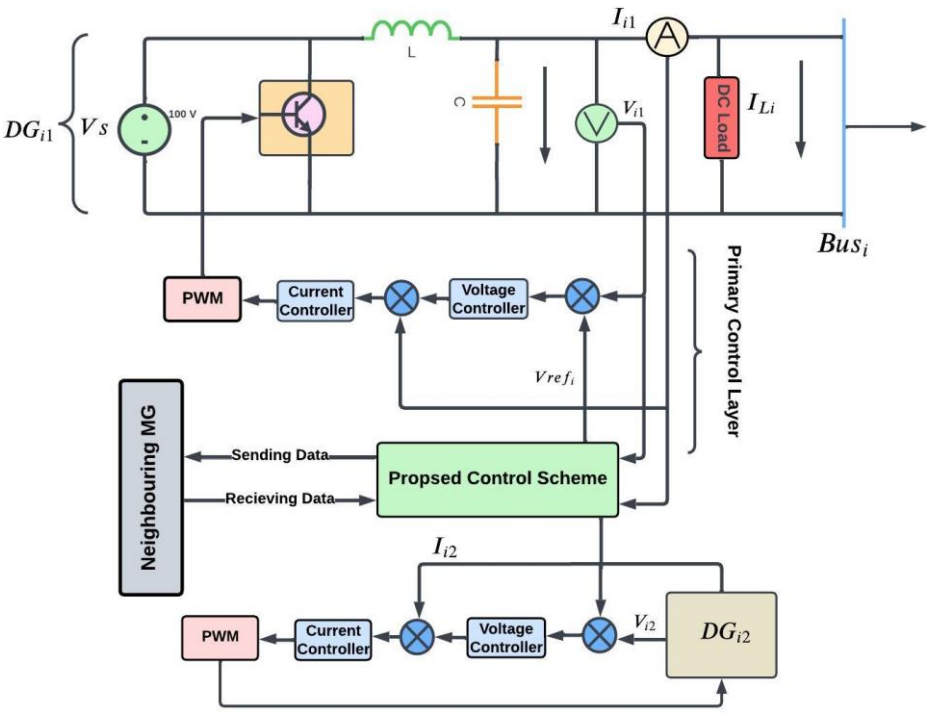

Fig. 3. The structure of each microgrid inside MGC.

the MG's primary control level shown in Fig.3 is driven by the reference voltage ($Vref$) from the global control layer, which includes the secondary and tertiary control layers. It effectively regulates the voltage and current levels of the MG. The voltage loop adjusts the DG's output voltage based on measured and reference voltages, while the current loop adjusts the DG's output current using measured and reference currents. These control loops enable the local control layer to achieve the primary objectives of the MG: maintaining stable output voltage and synchronizing the MG's output power with the load's requirements. This ensures overall MG stability, reliability, and efficient fulfilment of the load's power needs.

Table 1. Microgrids Parameters

Symbol	Value	Unit
Nominal Voltage	48	V
Converter Resistance	0.52	Ω
Converter Inductor	0.002	H
Converter Capacitor	0.005	F
Switching Frequency	20000	Hz
K_i and K_V	34	------
β(x10^{-6})	363,195,396,1931	------
Conductance	1	S
Sigma	*0.991*	------

In this study, the load resistances are set at 24Ω, 12Ω, 16Ω, and 9.6Ω, each with a nominal voltage of 48V for the MGs in the cluster, respectively. Despite the varying

loads, DC bus voltages fall within the acceptable range of 48.44V to 47.76V, as illustrated in Fig.4(a), and closely communicating MGs with the same rated currents (8A and 10A) converge their load currents to the equilibrium set point within an impressive 0.085 seconds, a notably faster convergence compared to [27], as depicted in Fig. 5(a). The load currents stabilize at 3.1 A, 3.1 A, 3.9 A, and 3.9 A, demonstrating the strength of the proposed control approach in ensuring precise current allocation between the clusters in the array. This precise current distribution dramatically reduces power loss. Subsequent subsections present various scenarios to assess the effectiveness of the proposed control method under different conditions.

5.1 Load Changes Scenario

In this scenario, load resistances in the MGs were modified at 1.5s and 2.5s, resulting in an increase in total load current from 13.9A to 22.4A and 28.4A, respectively, achieved by reducing resistances to 39% - 52.5% of their initial values. The system responded rapidly to these changes, as depicted in Fig. 4. Bus voltages (Vdc) were effectively maintained within 48.44V, 48.44V, 47.76V, and 47.7V from 1.5s to 2.5s. The rapid convergence of load currents (Idc) occurred within 0.085s during the intervals 0-1.5s and at 1.55s and 1.56s during the interval 1.5s-2.5s, as shown in Fig. 5. These results highlight the success of the proposed strategy in coordinating microgrids participating within the cluster.

Furthermore, average bus voltages (Vav) in the MG cluster were well-regulated within an acceptable range ($47.953V < Vav < 48.015V$) during steady-state operation, recovering rapidly to the standard limit after disturbances at 1.5s and 2.5s, as demonstrated in Fig. 4(b). The voltage tracking error, arising from deviations between voltage profiles and reference voltages of the buses, remained minimal (< 0.81V and 0.061V) during the load changes at 1.5s and 2.5s, as shown in Fig. 4(c). Additionally, key control objectives specified in (Eqs. (1) and (2)) were accurately achieved, as illustrated in Figs. 4(c), 4(d), and 5(b).

Notably, the number of triggering events was significantly reduced compared to previous studies in the literature, as evident in Fig. 6. This reduction stems from the minimal system error, which rarely exceeded the threshold value except at specific instants coinciding with load changes. This demonstrates the robustness of the event-trigger consensus method against disturbances like load changes and faults. Minor errors had negligible impact, as observed in Fig. 7. Referring to Fig. 6, the data sampling and transmitting instances decreased from exactly 14,000 times employing the time-triggering consensus algorithm to 88 times based on one-millisecond sampling intervals with the proposed technique.

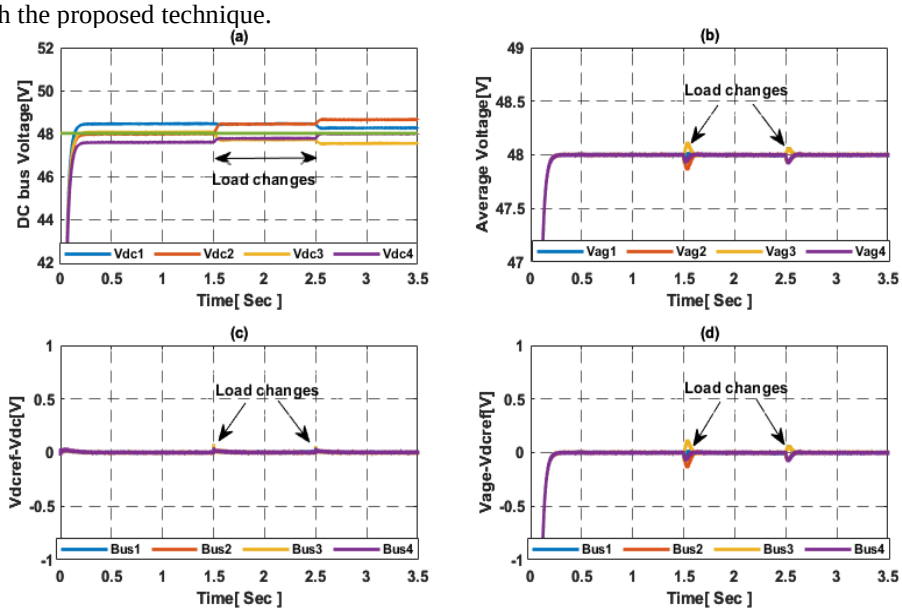

Fig.4. Scenario I (a) DC voltage, (b) Average voltage, (c) voltage regulation errors, and (d) Voltage observers (Eq. (2))

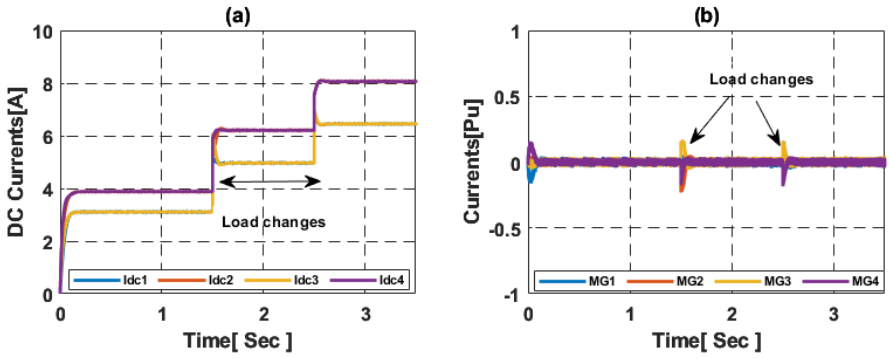

Fig.5. Scenario I (a) DC Current (b) Current Sharing errors (Eq. (1)).

To conclude, Figs. 4-5 illustrate the efficacy of the proposed scheme in accomplishing good voltage regulation within the range of 0.625-0.9% of all the MGs, precise currents sharing, and less communication interaction among MGs. These positively reflect on minimizing the likelihood of data congestion because the proposed control scheme allows microgrids in the cluster to operate appropriately without requiring continuous, extensive data interchange between them, as illustrated in Fig. 6.

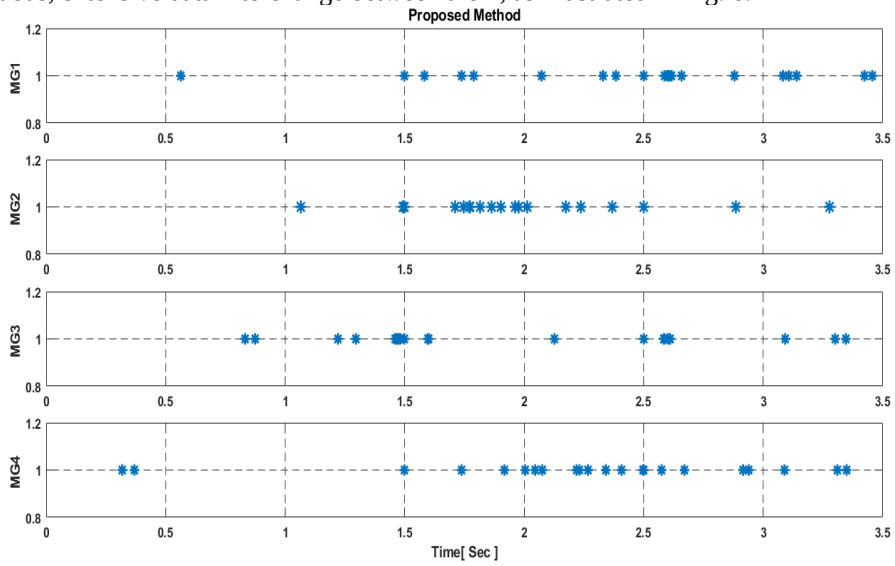

Fig.6. Triggering instants for each MG.

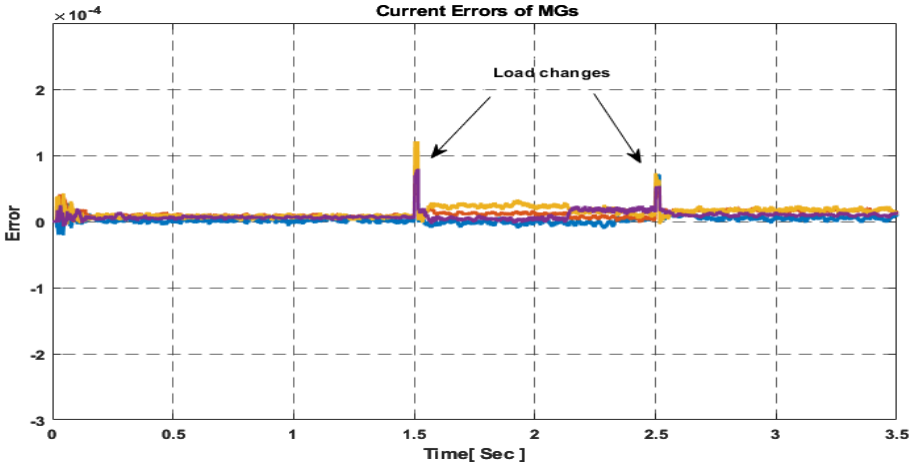

Fig.7. The error between the actual and last triggering currents.

5.2 Faults Scenario

In this Scenario, faults occur in MG2 and MG3 at 2s and 3s, respectively. The results reveal that such conditions have a limited impact on the system, as evident in Fig. 8(a), where DC bus voltages remain within standard limits. Additionally, load current

convergence occurs swiftly within the range of **0.01s-0.08s,** ensuring precise current sharing among participating MGs, as demonstrated in Fig. 9(a). The cluster's average voltages consistently fall within the range of 47.73V to 48.18V. The voltage tracking error of the buses remains within a range of 0.25V to -0.175V, as displayed in Fig. 4(c). Notably, the primary control objectives specified in (Eqs. (1) and (2)) are accurately achieved, as explained in Figs.8(d) and 9(b), respectively. Furthermore, it is noteworthy that triggering instances remain low and are minimally affected by minor system errors, as shown in Fig. 10. Under these concurrent conditions within the cluster, MG2 and MG3 temporarily suspend information sharing during the fault, as indicated in Fig. 10.

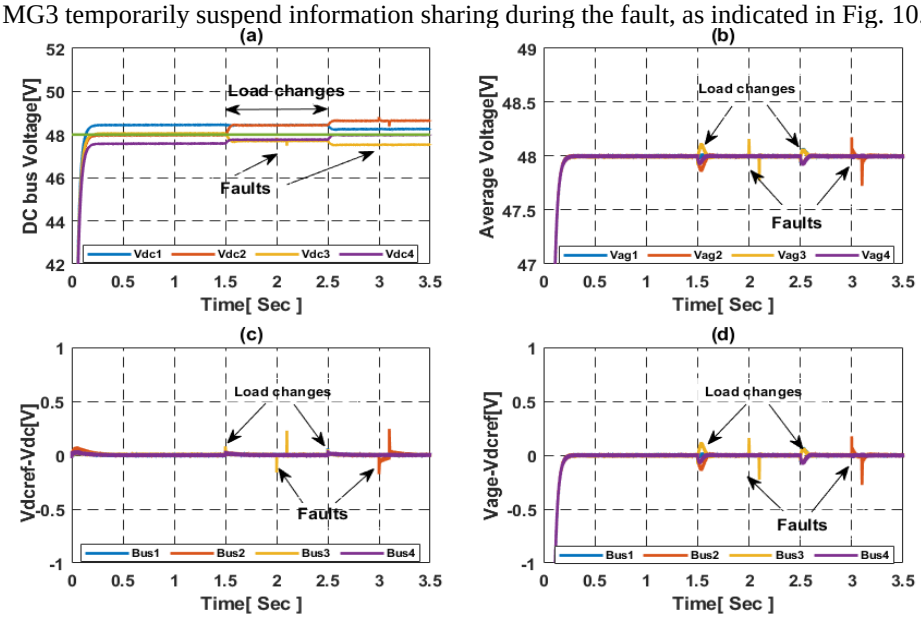

Fig.8. Scenario II (a) DC voltage (b) Average voltage (c) Voltage regulation errors (d) Voltage observers (Eq. (2)).

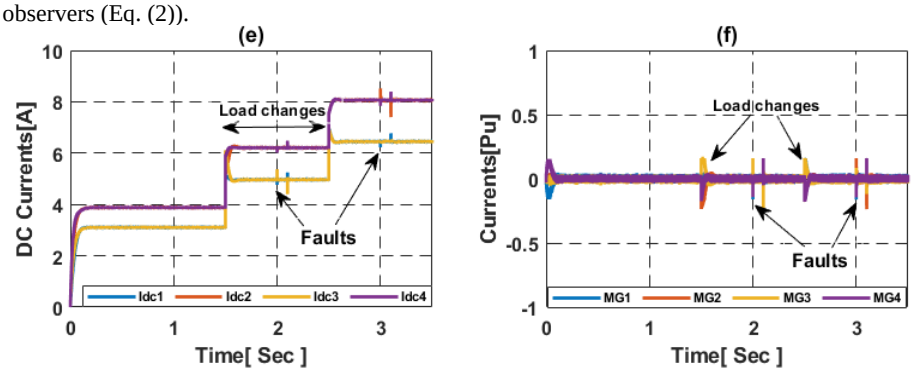

Fig.9. Scenario II (a) DC Current (b) Current Sharing errors (Eq. (1)).

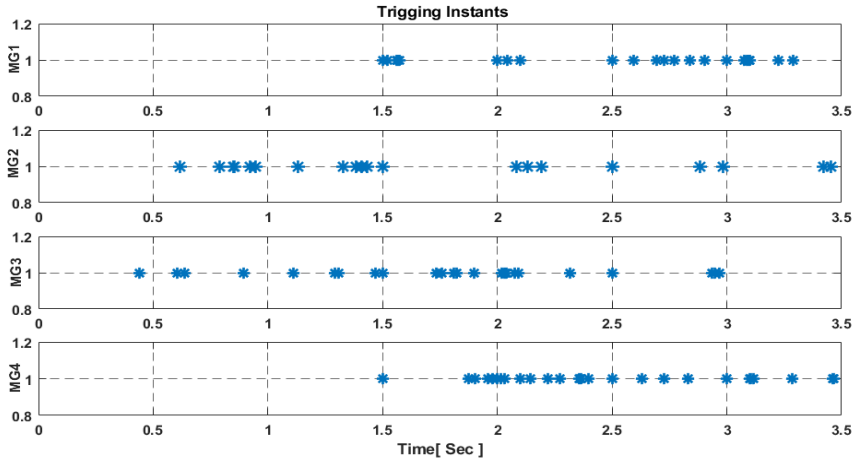

Fig.10. Triggering instants for each MG.

6. Comparison With the Existing Control Techniques

The proposed technique is compared to the existing event-trigger method [13]. One key advantage of this technique is its use of GWO in the primary control level, ensuring voltage regulation within the range of 47.6V to 48.35V from 1.5s to 2.5s. In contrast, the range of bus voltages in [30] was 47.1V to 49.5V at 1.5s and 42.8V to 51.76V at 2.5s. Additionally, load current convergence occurred at 0.085s during the interval 0-1.5s and then at 1.57s during the interval 1.5s-2.5s, both faster than the method proposed in [30].Another advantage is the proposed method's achievement of more accurate current sharing among MGs in the cluster compared to [30] The voltage tracking error remained below 0.1V and 0.05V even during load changes at 1.5s and 2.5s, a significant improvement over [30], where the error ranged from 1.5V to 5.39V. Furthermore, the proposed method requires fewer triggering instances than [30] Specifically, this method requires 88 instances (22, 19, 24, and 23). In comparison, DETC in [30] requires 201 instances (45+46+59+51), illustrating the robustness of the proposed event-trigger function, as shown in Fig.14 and Fig.15. Consequently, Zeno behavior is eliminated, reducing communication and making the proposed approach more efficient in both transient and steady-state stages.

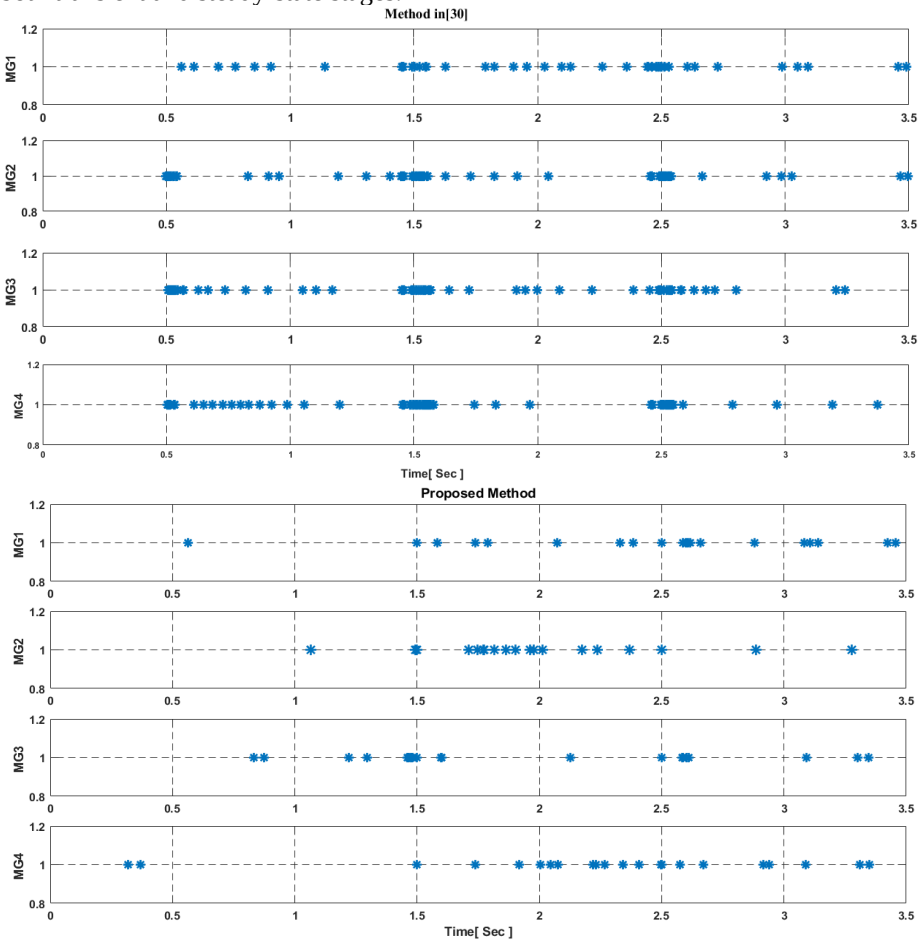

Fig.11 Triggering instants of method in [30] and the proposed method.

The comparison in Fig. 12 demonstrates that MDETC significantly outperforms the distributed event-triggered consensus algorithm presented in [30] in reducing communication requirements among MGs within the cluster, with only 88 triggering instants needed compared to 201. This underscores the feasibility of the proposed scheme in increasing the overall efficiency of the cluster by alleviating data congestion.

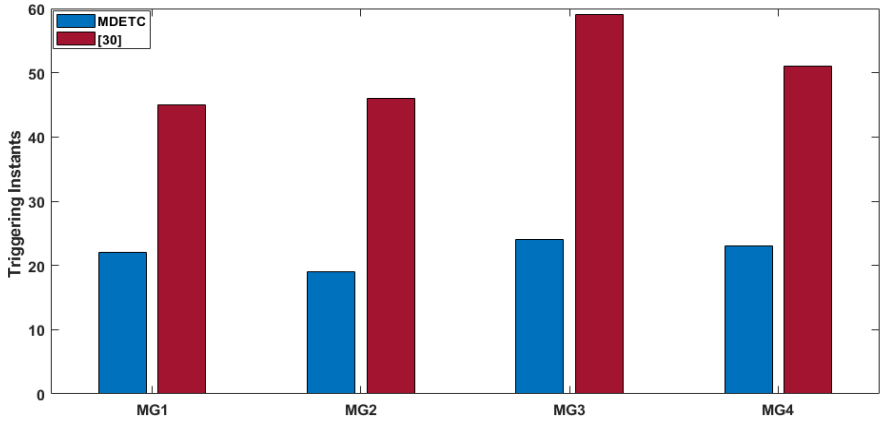

Fig.12. Comparison between the proposed control method and technique in [30].

7. Conclusion

This article presents the MDETC as a new control technique to boost the global control layer of a four-DC microgrid cluster. The proposed technique effectively addresses load changes, faults, PNP scenarios, and communication delays. Results demonstrate that integrating the GWO in the primary control level and a fixed-time consensus protocol in the second level successfully maintains DC voltage within standard limits, facilitates rapid recovery from voltage drops, and achieves precise proportional current sharing based on the maximum loading capacities among the MGs, with fast convergence rates within the cluster, thereby reducing cluster power losses. Moreover, average voltage observers converge optimally to the nominal voltage under critical operating conditions of the cluster. Furthermore, MDETC imposes strict triggering constraints, reducing the system's sensitivity to minor errors and minimizing the need for continuous interactions among MGs, thereby decreasing the likelihood of communication delays. Simulation results confirm the cluster's resilience to disturbances, validating the effectiveness of the control algorithm. Future work aims to enhance this algorithm by incorporating artificial neural networks (ANN) to predict parameters such as σ, ρ, c, and b based on the cluster's conditions, minimizing unnecessary interactions among MGs during steady states.

References

[1] Q. Xu, Y. Xu, Z. Xu, L. Xie, and F. Blaabjerg, “A Hierarchically Coordinated Operation and Control Scheme for DC Microgrid Clusters under Uncertainty,” *IEEE Trans Sustain Energy*, vol. 12, no. 1, 2021, doi: 10.1109/TSTE.2020.2991096.

[2] M. Glinkowski *et al.*, “Microgrids,” *Smart Grids: Clouds, Communications, Open Source, and Automation*, pp. 213–249, 2017, doi: 10.1201/b16908.

[3] O. Rezaei, O. Mirzapour, M. Panahazari, and H. Gholami, “Hybrid AC/DC Provisional Microgrid Planning Model Considering Converter Aging,” *Electricity*, vol. 3, no. 2, pp. 236–250, Jun. 2022, doi: 10.3390/electricity3020014.

[4] S. K. Sahoo, A. K. Sinha, and N. K. Kishore, “Control Techniques in AC, DC, and Hybrid AC-DC Microgrid: A Review,” 2018. doi: 10.1109/JESTPE.2017.2786588.

[5] Y. Han *et al.*, “Coordinated power control with virtual inertia for fuel cell-based DC microgrids cluster,” *Int J Hydrogen Energy*, vol. 44, no. 46, 2019, doi: 10.1016/j.ijhydene.2019.06.128.

[6] K. Thankanadar Saraswathi, G. v Swaminathan, and S. Periasamy, “Hybrid power management for DC microgrid cluster,” *Electric Power Systems Research*, vol. 199, no. May, p. 107454, 2021, doi: 10.1016/j.epsr.2021.107454.

[7] L. Meng *et al.*, "Review on Control of DC Microgrids and Multiple Microgrid Clusters," *IEEE J Emerg Sel Top Power Electron*, vol. 5, no. 3, 2017, doi: 10.1109/JESTPE.2017.2690219.

[8] A. Abhishek, S. Devassy, S. A. Akbar, and B. Singh, "Consensus Algorithm based Two-Level Control Design for a DC Microgrid," in *2020 IEEE International Conference on Power Electronics, Smart Grid and Renewable Energy, PESGRE 2020*, 2020. doi: 10.1109/PESGRE45664.2020.9070734.

[9] S. Moayedi and A. Davoudi, "Distributed Tertiary Control of DC Microgrid Clusters," *IEEE Trans Power Electron*, vol. 31, no. 2, 2016, doi: 10.1109/TPEL.2015.2424672.

[10] C. Wu, X. Hou, Y. Wang, X. Chen, and C. Liao, "SOC-featured Distributed Tertiary Control for Energy Management in DC Microgrid Clusters," in *2019 22nd International Conference on Electrical Machines and Systems, ICEMS 2019*, 2019. doi: 10.1109/ICEMS.2019.8922431.

[11] L. Ding, Q. L. Han, X. Ge, and X. M. Zhang, "An overview of recent advances in event-triggered consensus of multiagent systems," *IEEE Trans Cybern*, vol. 48, no. 4, 2018, doi: 10.1109/TCYB.2017.2771560.

[12] Z. G. Wu, Y. Xu, R. Lu, Y. Wu, and T. Huang, "Event-Triggered Control for Consensus of Multiagent Systems with Fixed/Switching Topologies," *IEEE Trans Syst Man Cybern Syst*, vol. 48, no. 10, 2018, doi: 10.1109/TSMC.2017.2744671.

[13] D. Pullaguram, S. Mishra, and N. Senroy, "Event-Triggered Communication Based Distributed Control Scheme for DC Microgrid," *IEEE Transactions on Power Systems*, vol. 33, no. 5, 2018, doi: 10.1109/TPWRS.2018.2799618.

[14] Z. Zhang *et al.*, "An Event-Triggered Secondary Control Strategy with Network Delay in Islanded Microgrids," *IEEE Syst J*, vol. 13, no. 2, 2019, doi: 10.1109/JSYST.2018.2832065.

[15] W. Meng, X. Wang, and S. Liu, "Distributed load sharing of an inverter-based microgrid with reduced communication," *IEEE Trans Smart Grid*, vol. 9, no. 2, 2018, doi: 10.1109/TSG.2016.2587685.

[16] C. Li, X. Yu, W. Yu, T. Huang, and Z. W. Liu, "Distributed Event-Triggered Scheme for Economic Dispatch in Smart Grids," *IEEE Trans Industr Inform*, vol. 12, no. 5, 2016, doi: 10.1109/TII.2015.2479558.

[17] Y. Fan, G. Hu, and M. Egerstedt, "Distributed Reactive Power Sharing Control for Microgrids with Event-Triggered Communication," *IEEE Transactions on Control Systems Technology*, vol. 25, no. 1, 2017, doi: 10.1109/TCST.2016.2552982.

[18] Zhongwen Li, Zhiping Cheng, Jikai Si, and Shuhui Li, "Distributed Event-Triggered Secondary Control for Average Bus Voltage Regulation and Proportional Load Sharing of DC Microgrid," *Journal of Modern Power Systems and Clean Energy* , 2021.

[19] B. Fan, J. Peng, Q. Yang, and W. Liu, "Distributed Periodic Event-Triggered Algorithm for Current Sharing and Voltage Regulation in DC Microgrids," *IEEE Trans Smart Grid*, vol. 11, no. 1, 2020, doi: 10.1109/TSG.2019.2926108.

[20] L. Xing, Q. Xu, F. Guo, Z. G. Wu, and M. Liu, "Distributed secondary control for DC microgrid with event-triggered signal transmissions," *IEEE Trans Sustain Energy*, vol. 12, no. 3, 2021, doi: 10.1109/TSTE.2021.3066334.

[21] Z. Chen, X. Yu, W. Xu, and G. Wen, "Modeling and Control of Islanded DC Microgrid Clusters with Hierarchical Event-Triggered Consensus Algorithm," *IEEE Transactions on Circuits and Systems I: Regular Papers*, vol. 68, no. 1, pp. 376–386, 2021, doi: 10.1109/TCSI.2020.3033432.

[22] S. Jena, N. P. Padhy, and J. M. Guerrero, "Decentralized Primary and Distributed Secondary Control for Current Sharing and Voltage Regulation in DC Microgrid Clusters with HESS," in *9th IEEE International Conference on Power Electronics, Drives and Energy Systems, PEDES 2020*, 2020. doi: 10.1109/PEDES49360.2020.9379838.

[23] S. Sahoo and S. Mishra, "An adaptive event-triggered communication-based distributed secondary control for DC microgrids," *IEEE Trans Smart Grid*, vol. 9, no. 6, 2018, doi: 10.1109/TSG.2017.2717936.

[24] P. Shafiee, M. Ahmadi, S. Najafi, Y. Batmani, and Q. Shafiee, "Event-Triggered Fully-Distributed Secondary Control of Islanded DC Microgrids Using Pre-defined Event Condition," in *2021 12th Power Electronics, Drive Systems, and Technologies Conference, PEDSTC 2021*, 2021. doi: 10.1109/PEDSTC52094.2021.9405952.

[25] P. Shafiee, Y. Khayat, Y. Batmani, Q. Shafiee, and J. M. Guerrero, "On the Design of Event-Triggered Consensus-Based Secondary Control of DC Microgrids," *IEEE Transactions on Power Systems*, vol. 37, no. 5, 2022, doi: 10.1109/TPWRS.2021.3136679.

[26] J. Savaliya, K. Patel, and A. Mehta, "Distributed Event-Triggered Sliding Mode Control for Voltage Synchronization of DC Microgrid Using Leader–Follower Consensus Protocol," in *Lecture Notes in Electrical Engineering*, 2020. doi: 10.1007/978-981-15-0226-2_3.

[27] S. A. Alavi, K. Mehran, Y. Hao, A. Rahimian, H. Mirsaeedi, and V. Vahidinasab, "A distributed event-triggered control strategy for dc microgrids based on publish-subscribe model over industrial wireless sensor networks," *IEEE Trans Smart Grid*, vol. 10, no. 4, 2019, doi: 10.1109/TSG.2018.2856893.

[28] J. Peng, B. Fan, Q. Yang, and W. Liu, "Distributed event-triggered control of dc microgrids," *IEEE Syst J*, vol. 15, no. 2, 2021, doi: 10.1109/JSYST.2020.2994532.

[29] Z. Chen, X. Yu, W. Xu, and G. Wen, "Modeling and Control of Islanded DC Microgrid Clusters with Hierarchical Event-Triggered Consensus Algorithm," *IEEE Transactions on Circuits and Systems I: Regular Papers*, vol. 68, no. 1, 2021, doi: 10.1109/TCSI.2020.3033432.

[30] J. Peng, B. Fan, Q. Yang, and W. Liu, "Distributed event-triggered control of dc microgrids," *IEEE Syst J*, vol. 15, no. 2, 2021, doi: 10.1109/JSYST.2020.2994532.

[31] Y. Y. Qian, A. V. P. Premakumar, Y. Wan, Z. Lin, Y. A. Shamash, and A. Davoudi, "Dynamic Event-Triggered Distributed Secondary Control of DC Microgrids," *IEEE Trans Power Electron*, vol. 37, no. 9, 2022, doi: 10.1109/TPEL.2022.3161967.

[32] N. Yan, G. Ma, T. Yan, S. Ma, and H. Zhao, "Research on the double-layer intra-day management and control method of ring structure microgrid cluster based on multi-time scale," *Energy Reports*, vol. 7, 2021, doi: 10.1016/j.egyr.2021.09.030.

[33] M. Islam, F. Yang, and M. Amin, "Control and optimisation of networked microgrids: A review," 2021. doi: 10.1049/rpg2.12111.

[34] C. Tian, K. Liu, and Z. Ji, "Adaptive event-triggered consensus of multi-agent systems with general linear dynamics," *Int J Syst Sci*, vol. 53, no. 8, 2022, doi: 10.1080/00207721.2021.2023687.

[35] S. Moayedi and A. Davoudi, "Distributed Tertiary Control of DC Microgrid Clusters," *IEEE Trans Power Electron*, vol. 31, no. 2, 2016, doi: 10.1109/TPEL.2015.2424672.

[36] Q. Liu, M. Ye, J. Qin, and C. Yu, "Event-triggered algorithms for leader-follower consensus of networked euler-lagrange agents," *IEEE Trans Syst Man Cybern Syst*, vol. 49, no. 7, 2019, doi: 10.1109/TSMC.2017.2772820.

[37] Z. H. A. Al-Tameemi, T. T. Lie, G. Foo, and F. Blaabjerg, "Optimal Coordinated Control Strategy of Clustered DC Microgrids under Load-Generation Uncertainties Based on GWO," *Electronics (Switzerland)*, vol. 11, no. 8, Apr. 2022, doi: 10.3390/electronics11081244.